Optimized Derivatization Procedure for Characterizing (Aminomethyl)phosphonic Acid Impurities by GC–MS

Kenley K. Ngim*, Jack Green, Joel Cuzzi, Marita Ocampo and **Zhengtian Gu**
Pharmaceutical & Analytical Development, Theravance, Inc., South San Francisco, CA 94080

Abstract

The use of (aminomethyl)phosphonic acid (AMPA) as a drug substance starting material required its structurally-related impurities to be characterized in order to understand the final outcome and effect. Samples of AMPA were reacted with *N,O*-bis(trimethylsilyl)trifluoroacetamide with 10% trimethylchlorosilane (BSTFA + 10% TMCS) to produce volatile N- and O-trimethylsilyl derivatives. The derivatives were then analyzed by positive electron impact ionization gas chromatography mass spectrometry (EI^+-GC–MS). Optimized reaction conditions (90°C, 150 min, 50 µL pyridine, 500 µL BSTFA + 10% TMCS) were obtained experimentally and with a design of experiment (DOE). This optimal derivatization procedure was applied to AMPA samples, resulting in the proposed structures of related impurities of AMPA.

Introduction

The use of (aminomethyl)phosphonic acid (AMPA) as a drug substance starting material prompted an evaluation of the fate and effect of its impurities. The presence of structurally-related impurities of AMPA that could undergo similar chemical modification to yield corresponding drug substance impurities would require stricter controls of impurities in the AMPA used as a starting material. Because the quality of AMPA is typically tested by methods which are not sufficiently discriminating or selective for individual impurities (e.g., titration, thin layer chromatography), the structures and the levels of its impurities are not known. Additionally, conventional techniques used in pharmaceutical laboratories for direct analysis [i.e., high-performance liquid chromatography-UV (HPLC-UV), gas chromatography (GC)] would be precluded for AMPA or its structurally similar impurities on the basis of low volatility, poor reversed-phase retention (due to its highly hydrophilic properties) and the absence of a suitable UV chromophore.

*Author to whom correspondence should be addressed: email ngim.kenley@gene.com.

Because AMPA is of interest as the major environmental degradation product of glyphosate herbicide (1–5), there are numerous analytical references available as a basis for determining its impurities (6–18). The direct analysis of AMPA was performed by ion chromatography (IC) followed by condensation nucleation light scattering detection (6), inductively coupled plasma mass spectrometry (ICP-MS) (7), and electrospray MS (8). Alternatively, AMPA was directly analyzed by capillary electrophoresis followed by electrospray MS (9), fluorescence detection (using fluorescein as a background fluorophore) (10), and electrochemiluminescence detection (11).

The indirect detection of AMPA involves derivatization to improve reversed phase retention, volatility or detection. For example, HPLC or IC with fluorescence detection followed the post-column reaction of AMPA with *o*-phthalaldehyde (12), as well as its pre-column reaction with 9-fluorenylmethyl chloroformate (13) and 4-chloro-7-nitrobenzofurazan (14). Alternatively, AMPA was analyzed by GC or GC–MS following its reaction with trifluoroacetic anhydride, trifluoroacetic acid and trimethyl orthoformate to produce an N-acyl, O-ester adduct (15) and with *N*-methyl-*N*-(*tert*-butyldimethylsilyl)trifluoroacetimide (MTBSTFA) (16,17) or *N,O*-bis(trimethylsilyl)trifluoroacetamide (BSTFA) with trimethylchlorosilane (TMCS) (18) to yield *N*- and/or *O*-trimethylsilyl (TMS) derivatives.

Due to the uncertain composition of AMPA samples and the desire to structurally elucidate AMPA impurities, an optimized silylation using BSTFA with TMCS followed by capillary GC with positive electron impact ionization (EI^+) MS analysis was pursued. The selection of BSTFA with TMCS was based on prior experience with this reagent combination, as well as the capability of TMCS to enhance the silyl donor strength of other silylating reagents (19). The advantages to this approach include the capability to derivatize both amine and phosphonate groups likely to be found in AMPA-related impurity structures, high selectivity and sensitivity that is intrinsic to GC–MS, and well-characterized EI^+ fragmentation mechanisms for TMS derivatives of AMPA and related aminoalkyl phosphonate compounds (18,20,21). The optimization of silylation parameters, using a combination of experimental iteration and a design of experiment (DOE), would assure a higher likelihood of observing

unknown AMPA-related impurities in real samples. Such extensive optimization was not pursued or necessarily required in previous silylations of AMPA or AMPA-related structures (16–18,20,21), because the analytes were known and/or available as an authentic sample prior to derivatization.

This article will present the results of optimizing the silylation conditions for AMPA and structurally characterizing AMPA impurities using the optimal parameters in combination with capillary GC–MS.

Experimental

Chemicals

AMPA (99%), sodium phosphate dibasic (minimum 99.0%), pyridine (anhydrous, 99.8%) and carbon tetrachloride (reagent grade, 99.9%) were purchased from Sigma-Aldrich (St. Louis, MO). The silylation reagents BSTFA + 10% TMCS and BSTFA + 1% TMCS were purchased from Pierce Biotechnology (Rockford, IL).

Instrumentation

Agilent 6890 Series GC with a 5973N quadrupole EI$^+$ (70 eV) mass selective detector was used (Wilmington, DE). The mass spectrometer was operated in selected ion monitoring (SIM) mode (*m/z* 73, 195) for method optimization, and full scan acquisition (*m/z* 50–550) was employed for the structural characterization of AMPA impurities. Prepared AMPA samples were injected (1 µL) in split mode (25:1) onto an Agilent HP-5, 30 m × 0.32 mm i.d., 1.0-µ film capillary column carrying a constant flow of helium (1.0 mL/min). The inlet temperature was set at 225°C. The oven temperature program consisted of an initial condition of 75°C held for 2 min, followed by an increase to 280°C at a rate of 20°C/min and a final hold time of 20 min. The transfer line temperature was set at 300°C. Temperature settings for the MS included 150°C (quadrupole) and 230°C (source).

Sample preparation

The optimal reaction parameters for derivatizing AMPA impurities are described in the following. Samples of AMPA (2.5 mg) were weighed into conventional 2-mL screw cap GC–HPLC autosampler vials, followed by the additions of BSTFA + 10% TMCS (500 µL) and pyridine (50 µL). The vials were capped and heated at 90°C for 2.5 h, followed by equilibration to room temperature (~5 min) and the addition of carbon tetrachloride diluent (1 mL). During this process, solid AMPA was observed initially, but it dissipated to yield a clear solution before the end of the reaction period.

Design of experiment

Optimal reaction parameters for AMPA derivatization were characterized with a split-plot DOE generated by JMP 7.0 (SAS, Cary, NC). The following factors (and defined ranges) were evaluated: the reaction time (50, 250 min), the reaction temperature (60, 120°C), the volume of pyridine (25, 100 µL), and the volume of BSTFA + 10% TMCS (250, 1000 µL). Responses measured in the experiment included: the peak area of the triple trimethylsi-

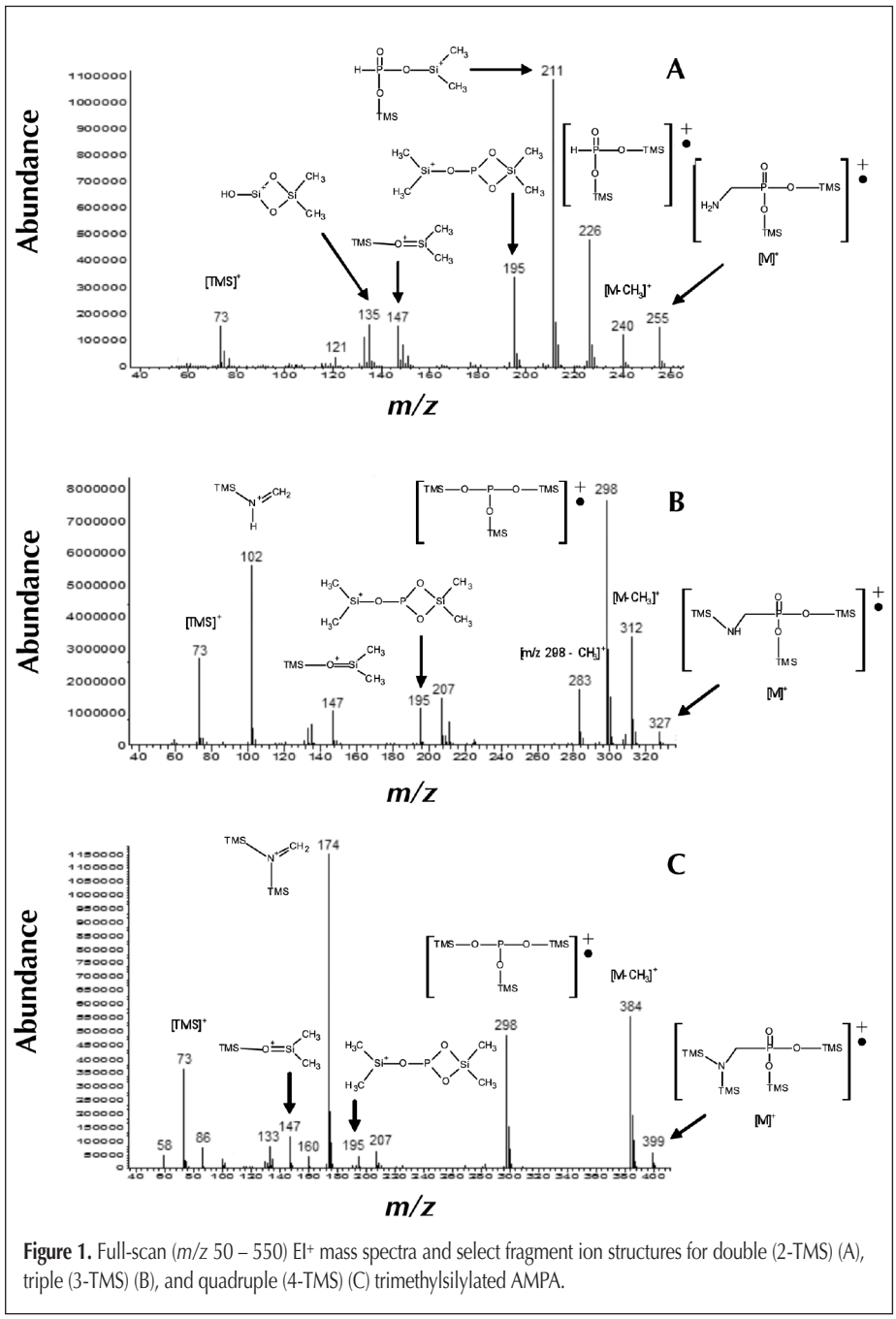

Figure 1. Full-scan (*m/z* 50 – 550) EI$^+$ mass spectra and select fragment ion structures for double (2-TMS) (A), triple (3-TMS) (B), and quadruple (4-TMS) (C) trimethylsilylated AMPA.

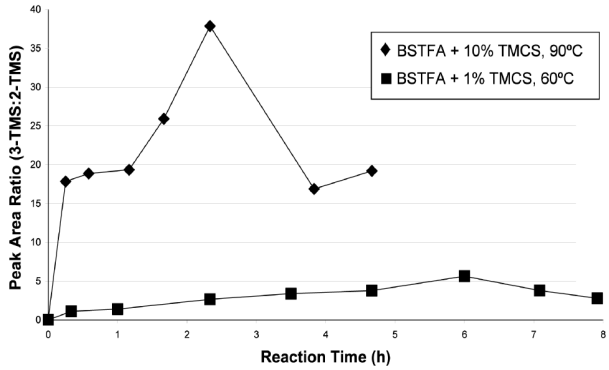

Figure 2. Comparative reactivity of AMPA towards BSTFA + 10% TMCS at 90°C and BSTFA + 1% TMCS at 60°C.

lylated (3-TMS) AMPA; the peak area of double trimethylsilylated (2-TMS) AMPA; the peak area ratio of 3-TMS:2-TMS AMPA; and the presence of residual AMPA solid in reacted samples. Each derivatized sample in the DOE experiment was subsequently diluted to a final volume of 1550 µL with carbon tetrachloride.

Results and Discussion

Reactivity of AMPA

Representative EI^+ mass spectra of observed AMPA derivatives along with proposed ions are shown in Figures 1A–1C. The identity of each AMPA derivative was assigned by interpreting its mass spectrum with respect to the expected molecular

Table I. Summary of Design of Experiment and Responses*

Whole Plots	Reaction Time (min)	Reaction Temp. (°C)	Pyridine Volume (µL)	Derivatizing Agent Volume (µL)	Peak Area 2-TMS AMPA	Peak Area 3-TMS AMPA	Peak Area Ratio 3-TMS:2-TMS AMPA	Solids Remain
1	250	120	25	1000	335448	84445582	251.7	No
1	250	120	100	250	223918	187746341	838.5	No
1	150	120	100	250	925943	242948165	262.4	No
1	50	120	100	1000	99779	398740728	3996.2	Yes
1	50	120	25	250	435399	348827698	801.2	Yes
2	250	60	100	1000	18617	135203029	7262.3	Yes
2	150	60	100	1000	19405	216182327	11140.5	Yes
2	250	60	25	250	40786	28608490	701.4	Yes
2	50	60	25	1000	10232	7280988	711.6	Yes
2	50	60	100	250	57242	41702466	728.5	Yes
3	50	99.3	100	250	37486	219648042	5859.5	Yes
3	150	99.3	25	1000	13795	210082843	15228.9	No
3	250	99.3	25	250	44658	247895887	5551.0	No
3	250	99.3	100	1000	55940	468074980	8367.4	No
3	50	99.3	25	1000	16303	192303198	11795.6	Yes
4	50	60	100	1000	14111	18286171	1295.9	Yes
4	150	60	25	250	153745	98431273	640.2	Yes
4	250	60	25	1000	5229	6599892	1262.2	Yes
4	250	60	100	250	38594	162751349	4217.0	Yes
4	50	60	25	250	54411	19194970	352.8	Yes

* The above design of experiment and responses is the basis for the final model summary (Table II) and predicted optimal silylation parameters (Table III).

Table II. Summary of Effects, Correlation Coefficients, and P-Values for the Final Model

	Probability Values for Effects									
Response	Temp.	Pyridine Volume	BSTFA + 10% TMCS Volume	Time * Temp.	Temp. * Pyridine Volume	Temp. * Temp.	Time	Time * Time	Correlation Coefficient	P Value
2-TMS AMPA Peak area	0.0256	0.9610	0.3121	0.9061	0.9914	0.0536	0.9424	0.2748	0.71	< 0.0001
3-TMS AMPA Peak area	0.0319	0.2432	0.7202	0.3030	0.8649	0.0830	0.8871	0.6436	0.68	< 0.0001
Peak Area Ratio (3-TMS:2-TMS AMPA)	0.4979	0.3574	0.0180	0.3175	0.1171	0.1065	0.9664	0.0177	0.85	< 0.0001
Unreacted AMPA	< 0.0001	0.9131	0.9177	< 0.0001	0.8408	< 0.0001	< 0.0001	0.0177	0.93	< 0.0001

Note: This final model summary is derived from the design of experiment and responses summarized in Table I.

weight and elution order. The key mass spectral feature for distinguishing AMPA derivatives is the cleavage of the alkyl phosphonate bond. The resultant trimethylsilylimine fragment ions $(TMS\text{-}NH{=}CH_2)^+$ (*m/z* 102) and $[(TMS)_2N{=}CH_2]^+$ (*m/z* 174) are characteristic of the 3-TMS and the quadruple trimethylsilylated (4-TMS) derivatives of AMPA, respectively; the corresponding fragment ion for the 2-TMS derivative ($[NH = CH_2]^+$) is below the mass detection threshold. Another important feature of the mass spectrum for each AMPA derivative is the desmethyl fragment ion ($[M - 15]^+$), which is useful for verifying the molecular ion assignment. Both attributes will be revisited in the discussion of the structural characterization of AMPA impurities.

The AMPA derivatives exhibit common fragment ions, which is the basis for the chosen SIM ions. These include fragment ions which are generic to TMS derivatives (e.g., *m/z* 73 ($[TMS]^+$), *m/z* 147 ($[TMS\text{-}O{=}Si(CH_3)_2]^+$ [22]) and one that is specific to trimethylsilylated phosphonates (e.g., *m/z* 195 [20]). Other proposed fragment ion structures (*m/z* 135, 195, 211, 226, 298) are consistent with the previously reported fragment ion identities and fragmentation mechanisms for several trimethylsilylated alkyl and aminoalkyl phosphonates (20).

The primary product of the reaction of AMPA is the 3-TMS derivative, including silylation of both phosphonate hydroxyls and a single silylation of its amine group. The 2-TMS derivative, comprised of silylated phosphonate hydroxyls only, was also observed. The fragmentation and relative ion abundance for 2-TMS and 3-TMS AMPA are consistent with previously reported EI^+ mass spectra for each derivative (20). The 4-TMS AMPA derivative is observed only intermittently and in relatively low abundance, which is attributed to steric constraints of a second N-silylation. The 3-TMS AMPA derivative is targeted in method optimization studies to ensure both greater robustness and control of the silylation reaction. Consequently, the 3-TMS:2-TMS AMPA peak area ratio was adopted as a quantitative measure of reaction completion, as well as for correcting MS response variability.

Table III. Optimal Reaction Parameters Predicted for Each Response Using Final Model Effects*

Response	Reaction Temp. (°C)	Reaction Time (min)	BSTFA + 10% TMCS Volume (µL)	Pyridine Volume (µL)
2-TMS AMPA†	79.9	50	1000	100
3-TMS AMPA†	106.4	99.6	1000	100
Peak Area Ratio‡	86.7	151.4	1000	100
Unreacted AMPA	120	250	1000	100

* Predictions are derived from the design of experiment and responses summarized in Table I.
† Peak Area ‡ 3-TMS AMPA –2-TMS AMPA

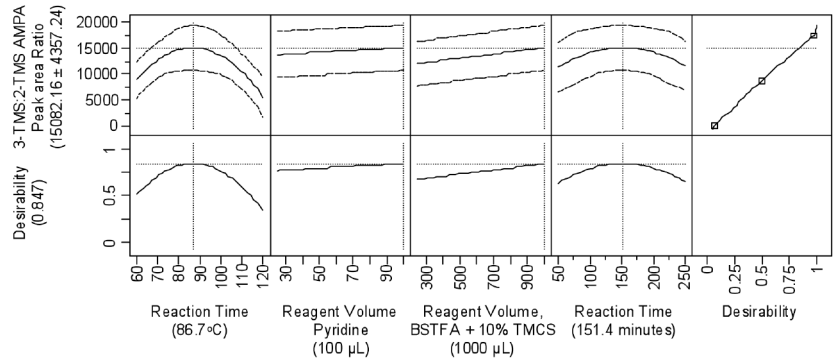

Figure 3. Desirability plots showing the effect of reaction parameters on the peak area ratio of triple trimethylsilylated to double trimethylsilylated (3-TMS–2-TMS) AMPA.

Table IV. Summary of Proposed Impurities Observed in AMPA

	Impurity	Retention Time	[M]+ (*m/z*)	MW (Da)	Vendor 1*	Vendor 2*	Vendor 3*
a	Phosphoric acid (3-TMS)	7.6 min	314	98	+	+	+
b1	Ethylene-AMPA (2-TMS)	8.4 min	281	137	+	+	+
c	R_1-AMPA (3-TMS)†	9.5 min	422	206	+	+	+
d	Ethyl-AMPA (3-TMS)	9.6 min	355	139	–	+	+
b2	Ethylene-AMPA (3-TMS)	9.8 min	353	137	+	+	+
e	Propyl-AMPA (3-TMS)	10.5 min	369	153	+	+	–
f	R_2-AMPA (3-TMS)†	11.1 min	443	227	+	+	–

* Vendor 1 (Aldrich) data obtained from single AMPA lot (same as that used for method optimization). Vendor 2 (private supplier) data obtained from single AMPA lot. Vendor 3 (private supplier) data obtained from three AMPA lots, each showing same impurity profile.
† R_1 = 96 Da; R_2 = 117 Da

Development and optimization of silylation procedure

The effectiveness of this silylation procedure for structurally-related AMPA impurities would be inferred by using AMPA itself. Effective derivatization temperature conditions for AMPA were determined by analyzing timed samples that were reacted as follows: BSTFA + 1% TMCS (500 µL), pyridine (50 µL), 60°C; and BSTFA + 10% TMCS (500 µL), pyridine (50 µL), 90°C. Plots of reaction time versus 3-TMS:2-TMS peak area ratio are presented in Figure 2. The reaction with BSTFA + 10% TMCS for 140 min at 90°C produced a 38:1 ratio, corresponding to a 97% conversion to 3-TMS AMPA. By contrast, a maximum ratio of just 5:1 (equivalent to 80% conversion) was achieved with BSTFA + 1% TMCS reacted at 60°C. Higher sample throughput, as well as the likelihood of increased sensitivity and a simplified chromatographic profile (i.e., fewer partially silylated derivatives for the same analyte), led to the choice of BSTFA + 10% TMCS.

To further optimize the silylation conditions, a DOE was employed. It was meant to evaluate the significance and cumulative impact of reaction parameters, which

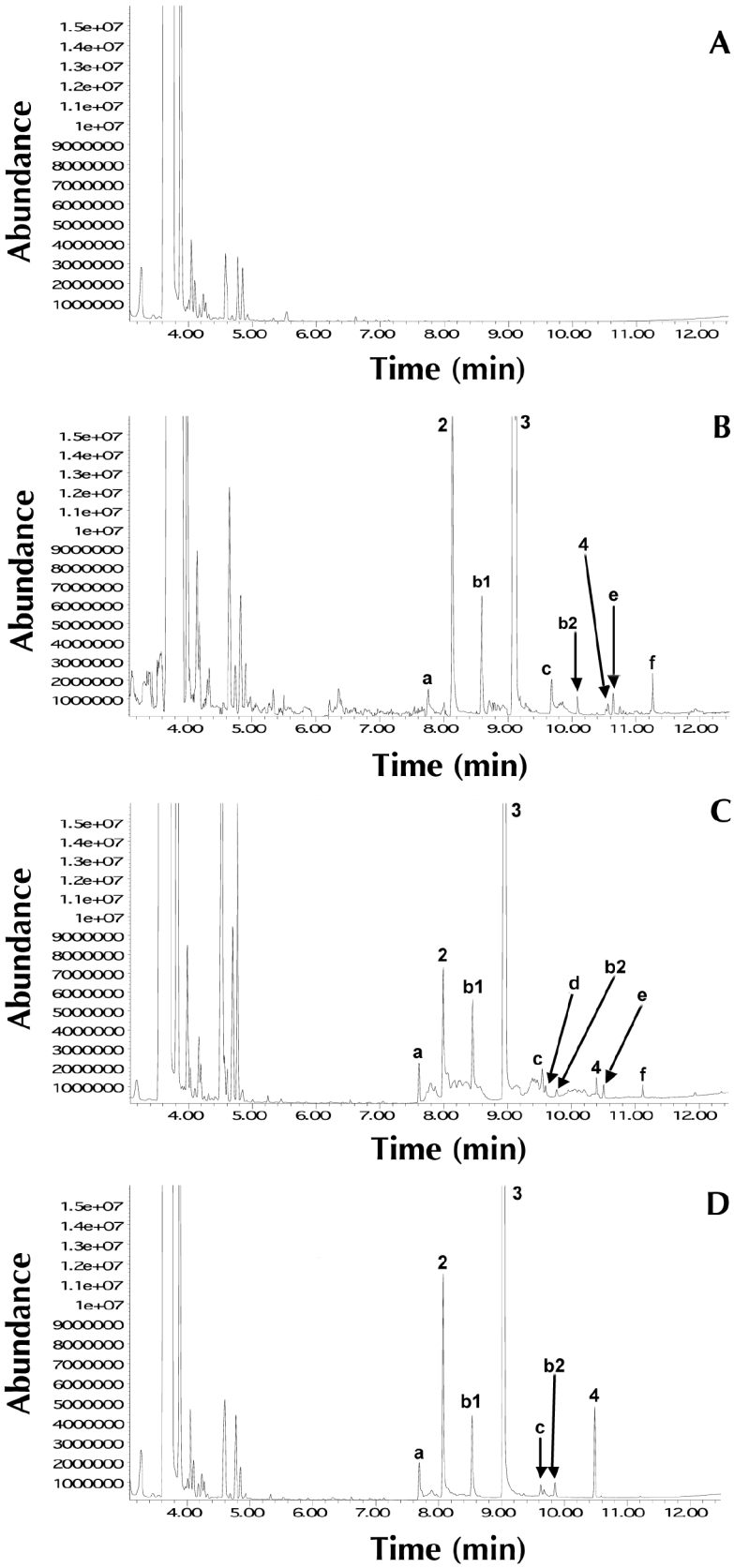

Figure 4. Full-scan total ion chromatograms of derivatized preparations, including reagent blank (A) and AMPA samples from Vendor 1 (B), Vendor 2 (C), and Vendor 3 (D). Impurity peaks are labeled (a, b1, c, d, b2, e, f), as are peaks corresponding to double (2), triple (3) and quadruple (4) trimethylsilylated AMPA. Refer to Table IV for the correlation of proposed impurity peak identities.

may have been overlooked or otherwise inadequately examined during method development. The DOE and corresponding response data for each of 20 prepared samples are included in Table I. The final model was established iteratively by rejecting effects for which probability values exceeded 0.2 in each response. The effects, P values and coefficient of determinations (r^2) for the final model fit are summarized in Table II. The P value for the model fit of each response was much less than 0.05, indicating that each response is a statistically significant measure of AMPA derivatization. Each response exhibited an acceptable linear fit.

Since the 3-TMS:2-TMS AMPA peak area ratio is the most meaningful response, its desirability plot (Figure 3) was the basis for verifying the silylation conditions. The predicted optimal reaction temperature (86.7°C) and reaction time (151.4 min) led to the adoption of 90°C and 150 min as the final silylation conditions. The insignificant change in response exhibited in the desirability plots for the volume of either reagent suggests that these parameters are robust within the evaluated ranges. As a result, the reagent volumes used in method development (500 µL BSTFA + 10% TMCS, 50 µL pyridine) were retained. Refer to Table III for a summary of optimal silylation parameters predicted for each response. The DOE also confirmed that reaction conditions established in method development were already very close to being optimal. The optimal reaction conditions are similar though better defined than parameters that were previously employed for silylating AMPA and AMPA-related compounds with BSTFA and TMCS (80°C, 15 min – 4 h [18]).

Because silyl derivatives are generally considered to be sensitive to moisture (19), the decomposition of 3-TMS AMPA was characterized from samples that were reinjected over the course of approximately 10 h. The plot of Storage Time (h) versus ln(3-TMS AMPA peak area) exhibited a linear response ($y = -0.0467x + 19.625$, $r^2 = 0.911$), resulting in a 5 h stability allowance that would ensure at least 80% of the initial 3-TMS AMPA would be present at the time of GC–MS analysis.

Structural characterization of AMPA impurities

Samples of AMPA from three vendors were silylated with the optimized reaction conditions and analyzed by full scan GC–MS. Total ion chromatograms (TIC) presented in Figure 4 exhibit as many as seven AMPA impurity peaks. Representative mass spectra for each impurity peak, including key ion structures, are shown in

Figures 5A–5G. A summary of proposed AMPA impurities, including the molecular weight, molecular ion and occurrence in AMPA from three sources, is shown in Table IV. Phosphoric acid (7.6 min) was observed as its triple silylated derivative and its identity was confirmed against a prepared standard.

The remaining impurities consist of alkyl-substituted AMPA structures, which were proposed from the assigned molecular and trimethylsilylimine fragment ions, as well as from similarities in fragmentation to the AMPA derivatives or other trimethylsilylated aminoalkyl phosphonates (20,21). For impurity spectra with weak molecular ion intensity (Figures 5B, 5C, 5F, and 5G), the assignment was confirmed or based on the expected occurrence of its desmethyl fragment ion. The position of AMPA substitution (i.e., N or

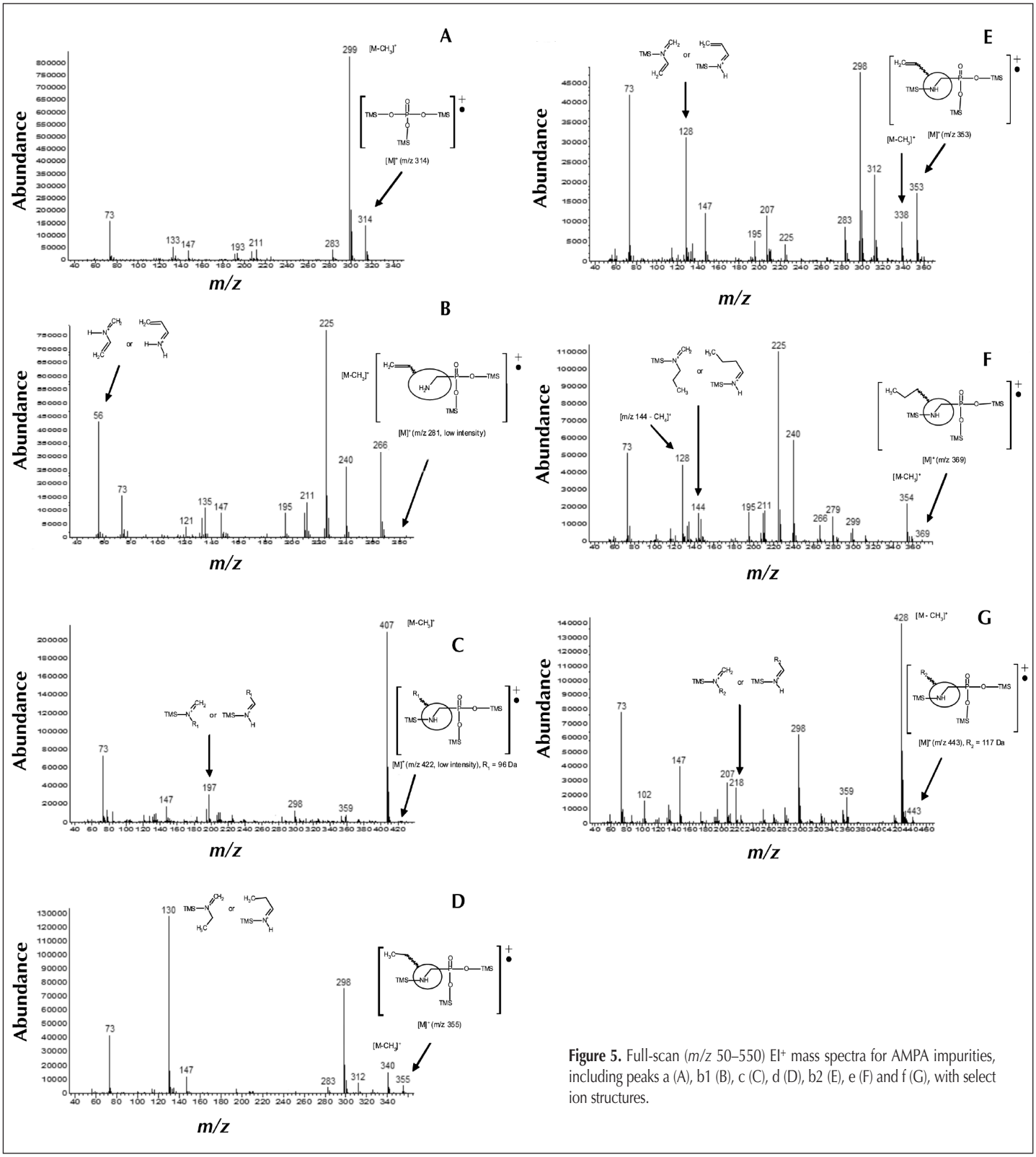

Figure 5. Full-scan (*m/z* 50–550) EI+ mass spectra for AMPA impurities, including peaks a (A), b1 (B), c (C), d (D), b2 (E), e (F) and f (G), with select ion structures.

C1) was undetermined for each impurity, as $(TMS\text{-}NR{=}CH_2)^+$ and $(TMS\text{-}NH{=}CHR)^+$ trimethylsilylimine fragments are both possible. An ethylene-AMPA impurity was observed as a 2-TMS (8.4 min) and 3-TMS (9.8 min) derivative, whereas R_1-AMPA (9.5 min), ethyl-AMPA (9.6 min), propyl-AMPA (10.5 min) and R_2-AMPA (11.1 min) were observed only as 3-TMS derivatives. The structures of sidechains R_1 (96 Da) and R_2 (117 Da) were undetermined. The absence of multiple derivative species for all impurities except ethylene-AMPA showed that the silylation parameters were highly effective and selective for AMPA-related impurities.

The full identification of the proposed AMPA-related impurities is still needed, which would resolve the uncertainty in the position of AMPA substitution. Considering that the availability of authentic standards for the proposed structures is limited, this would likely require isolation and more definitive characterization (e.g., NMR). However, this was beyond the scope and intended purpose of this work.

Conclusions

An effective silylation procedure employing BSTFA + 10% TMCS was developed, optimized, and implemented for the derivatization and structural characterization of AMPA impurities. Optimal reaction parameters (90°C, 150 minutes, 50 µL pyridine, 500 µL BSTFA + 10% TMCS) were determined by a combination of experimental iterations and a DOE. The derivatization of AMPA samples led to the characterization of structurally similar impurities, including phosphoric acid and alkyl-substituted AMPA structures. Since the reaction of aminoalkyl phosphonate impurities to corresponding drug substance impurities is feasible, this methodology offers an effective means of assessing and controlling the quality of AMPA used as a pharmaceutical starting material.

Acknowledgments

The authors thank Dr. Jyanwei Liu (formerly of Theravance, Inc.) and Drs. Junning Lee and Jayprakasam Bolleddula (Theravance, Inc.) for providing useful suggestions, which led to an understanding of potential AMPA impurity structures and the adopted analytical testing strategy.

References

1. K. Grunewald, W. Schmidt, C. Unger, and G. Hanschmann. Behavior of glyphosate and aminomethylphosphonic acid (AMPA) in soils and water of reservoir Radeburg II catchment (Saxony/Germany). *J. Plant Nutr. Soil Sci.* **164:** 65–70 (2001).
2. L. Simonsen, I.S. Fomsgaard, B. Svensmark, and N.H. Spliid. Fate and availability of glyphosate and AMPA in agricultural soil. *J. Environ. Sci. Health, Part B* **43:** 365–375 (2008).
3. D. Landry, S. Dousset, J-C. Fournier, and F. Andreux. Leaching of glyphosate and AMPA under two soil management practices in Burgundy vineyards (Vosne-Romanée, 21-France). *Environ. Pollut.* **138:** 191–200 (2005).
4. F. Botta, G. Lavison, G. Couturier, F. Alliot, E. Moreau-Guigon, N. Fauchon, B. Guery, M. Chevreuil, and H. Blanchoud. Transfer of glyphosate and its degradate AMPA to surface waters through urban sewerage systems. *Chemosphere* **77:** 133–139 (2009).
5. J. Kjaer, P. Olsen, M. Ullum, and R. Grant. Leaching of glyphosate and amino-methylphosphonic acid from Danish agricultural field sites. *J. Environ. Qual.* **34:** 608–620 (2005).
6. J. You and J.A. Korapchak. Condensation nucleation light scattering detection with ion chromatography for direct determination of glyphosate and its metabolite in water. *J. Chromatogr. A* **989:** 231–238 (2003).
7. M. Popp, S. Hann, A. Mentler, M. Fuerhacker, G. Stingeder, and G. Koellensperger. Determination of glyphosate and AMPA in surface and waste water using high-performance ion chromatography coupled to inductively coupled plasma dynamic reaction cell mass spectrometry (HPIC–ICP–DRC–MS). *Anal. Bioanal. Chem.* **391:** 695–699 (2008).
8. K.H. Bauer, T.P. Knepper, A. Maes, V. Schatz, and M. Voihsel. Analysis of polar organic micropollutants in water with ion chromatography–electrospray mass spectrometry. *J. Chromatogr. A* **837:** 117–128 (1999).
9. L. Goodwin, J.R. Startin, B.J. Keely, and D.M. Goodall. Analysis of glyphosate and glufosinate by capillary electrophoresis–mass spectrometry utilising a sheathless microelectrospray interface. *J. Chromatogr. A* **1004:** 107–119 (2003).
10. S.Y. Chang and C-H. Liao. Analysis of glyphosate, glufosinate and aminomethylphosphonic acid by capillary electrophoresis with indirect fluorescence detection. *J. Chromatogr. A* **959:** 309–315 (2002).
11. H.Y. Chiu, Z.Y. Lin, H.L. Tu, and C.W. Whang. Analysis of glyphosate and aminomethylphosphonic acid by capillary electrophoresis with electrochemiluminescence detection. *J. Chromatogr. A* **1177:** 195–198 (2008).
12. E. Mallat and D. Barceló. Analysis and degradation study of glyphosate and of aminomethylphosphonic acid in natural waters by means of polymeric and ion-exchange solid-phase extraction columns followed by ion chromatography–post-column derivatization with fluorescence detection. *J. Chromatogr. A* **823:** 129–136 (1998).
13. E. Le Fur, R. Colin, C. Charreteur, C. Dufau, and J.J. Peron. Determination of glyphosate herbicide and aminomethylphosphonic acid in natural waters by liquid chromatography using pre-column fluorogenic labeling. Part I : Direct determination at the 0.1 µg/L level using FMOC. *Analusis* **28:** 813–818 (2000).
14. R. Colin, E. Le Fur, C. Charreteur, C. Dufau, and J.J. Peron. Determination of glyphosphate herbicide and (aminomethyl)phosphonic acid (AMPA) in water by liquid chromatography and fluorescence detection. Part II : Direct determination using pre-column derivatization with NBD-Cl. *Analusis* **28:** 819–824 (2000).
15. Z.H. Kudzin, D.K. Gralak, J. Drabowicz, and J. Luczak. Novel approach for the simultaneous analysis of glyphosate and its metabolites. *J. Chromatogr. A* **947:** 129–141 (2002).
16. N. Tsunoda. Simultaneous determination of the herbicides glyphosate, glufosinate and bialaphos and their metabolites by capillary gas chromatography—ion-trap mass spectrometry. *J. Chromatogr.* **637:** 167–173 (1993).
17. H.A. Moye and C.L. Deyrup. A simple single-step derivatization method for the gas chromatographic analysis of the herbicide glyphosate and its metabolite. *J. Agric. Food Chem.* **32:** 192–195 (1984).
18. D.J. Harvey and M.G. Horning. Derivatives for the characterization of alkyl- and aminoalkylphosphonates by gas chromatography and gas chromatography-mass spectrometry. *J. Chromatogr.* **79:** 65–74 (1973).
19. D.R. Knapp. Handbook of Analytical Derivatization Reactions. Wiley-Interscience, New York, NY, 1979, p. 10.
20. D.J. Harvey and M.G. Horning. The mass spectra of the trimethylsilyl derivatives of some alkyl and aminoalkyl phosphonates. *Org. Mass Spectrom.* **9:** 111–124 (1974).
21. D.J. Harvey and M.G. Horning. The mass spectra of the trimethylsilyl esters of acetyl, schiff base and isothiocyanate derivatives of some aminoalkylphosphonic acids. *Org. Mass Spectrom.* **9:** 955–969 (1974).
22. J.L. Little. Artifacts in trimethylsilyl derivatization reactions and ways to avoid them. *J. Chromatogr. A* **844:** 1–22 (1999).

Manuscript received November 19, 2009;
revision received February 16, 2010